EUROFUSION WPMST1-PR(15) 13808

J Rosato et al.

A table of Balmer gamma line shapes for the diagnostic of magnetic fusion plasmas

Preprint of Paper to be submitted for publication in
Journal of Quantitative Spectroscopy and Radiative Transfer

This work has been carried out within the framework of the EUROfusion Consortium and has received funding from the Euratom research and training programme 2014-2018 under grant agreement No 633053. The views and opinions expressed herein do not necessarily reflect those of the European Commission.

This document is intended for publication in the open literature. It is made available on the clear understanding that it may not be further circulated and extracts or references may not be published prior to publication of the original when applicable, or without the consent of the Publications Officer, EUROfusion Programme Management Unit, Culham Science Centre, Abingdon, Oxon, OX14 3DB, UK or e-mail Publications.Officer@euro-fusion.org

Enquiries about Copyright and reproduction should be addressed to the Publications Officer, EUROfusion Programme Management Unit, Culham Science Centre, Abingdon, Oxon, OX14 3DB, UK or e-mail Publications.Officer@euro-fusion.org

The contents of this preprint and all other EUROfusion Preprints, Reports and Conference Papers are available to view online free at http://www.euro-fusionscipub.org. This site has full search facilities and e-mail alert options. In the JET specific papers the diagrams contained within the PDFs on this site are hyperlinked

A table of Balmer γ line shapes for the diagnostic of magnetic fusion plasmas

J. Rosato, H. Bufferand, M. Koubiti, Y. Marandet, R. Stamm

Aix-Marseille Université, CNRS, PIIM UMR 7345, F-13397 Marseille, France

Abstract

Spectral profiles of the Dγ line have been calculated in magnetic fusion plasma conditions for diagnostic purposes. This article reports on the elaboration of a table devoted to spectroscopic applications in the divertor of the ASDEX-Upgrade tokamak that extends an already existing database. An overview of the method, together with the physics underlying the broadening of spectral lines, is given. A special emphasis is put on the role of the simultaneous action of the Stark and Zeeman effects.

Keywords:

1. Introduction

A research campaign that involves medium size tokamaks (MST1 project) has been led last year in order to broaden the already existing experimental and theoretical databases supporting the preparation of ITER and the subsequent demonstration power plant DEMO. In this article, we report on the development of a spectroscopic database for the interpretation of hydrogen Balmer lines in conditions of high-density recombining divertor plasmas (viz. $N_e = 10^{14}$ cm^{-3} and higher), following previous works performed at Garching (ASDEX-Upgrade tokamak [1]). At such high-density plasma conditions, the spectral lines with a high principal quantum number n (say, of the order of 10) are affected by Stark broadening and can be used as a probe of the electron density (passive spectroscopy), e.g. [2, 3, 4, 5, 6, 7, 8, 9, 10]. An analysis of lines with a moderate quantum number such as Dγ ($n = 5$) is more intricate, because the Stark broadening can be of the same order as the Doppler broadening and it can be affected by ion dynamics. Furthermore, the presence of a strong magnetic field (of the order of several teslas) results

in an alteration of the energy level structure, which is not straightforward even for hydrogen due to the simultaneous action of the magnetic field and the plasma's microscopic electric field (for a recent discussion, e.g. [11]). The spectroscopic data used in [1] were obtained from the so-called model microfield method (MMM) [12] (it provides an analytical formula for the line shape, e.g. [13] for details). We present here an extension that provides a finer grid and that accounts for the presence of a magnetic field. Our table of line shapes has been calculated from a computer simulation method [14], following early works [15, 16]. The method involves a numerical integration of the time-dependent Schrödinger equation for the hydrogen wave function under the influence of a fluctuating electric field (the plasma microfield), the latter being obtained from a particle simulation. In principle, this method can be used as a benchmark for analytical line shape models involving specific physical approximations (for a comprehensive review, e.g. [17]). Our code has been tested and validated by confrontation against other codes at the "Spectral Line Shapes in Plasmas Code Comparison Workshop" (SLSP) [18]. The paper is organized as follows: section 2 gives an overview on the Stark line shape formalism, section 3 presents the simulation method, and section 4 gives an application of the database to the calculation of a spectrum observed in a "virtual" plasma background simulated from a transport code (synthetic diagnostics).

2. Line broadening formalism

We give a summary of the formalism, along the lines of [11]. According to classical textbooks on spectroscopy (e.g. [19]), the spectral profile of an atomic line, $I(\omega, \mathbf{n})$, is given in terms of the line profile in the atom's frame of reference $I_0(\omega, \mathbf{n})$ by Doppler convolution

$$I(\omega, \mathbf{n}) = \int d^3v f(\mathbf{v}) I_0(\omega - \omega_0 \mathbf{v} \cdot \mathbf{n}/c, \mathbf{n}). \tag{1}$$

Here, ω_0 is the central angular frequency of the line under consideration, ω and $\mathbf{n}$ denote the frequency and the observation direction, and $f(\mathbf{v})$ is the atomic velocity distribution (VDF). For Maxwellian VDF, the line shape is a Gaussian function if there is no broadening mechanism in the atom's frame of reference [i.e. when $I_0(\omega, \mathbf{n}) \equiv \delta(\omega - \omega_0)$] and a Voigt function if natural broadening is retained. In the general case, $I_0(\omega, \mathbf{n})$ is proportional

to the Fourier transform of the atomic dipole autocorrelation function $C_{\mathbf{n}}(t)$, a quantity described in the framework of quantum mechanics

$$I_0(\omega, \mathbf{n}) = \frac{1}{\pi}\mathrm{Re}\int_0^\infty dt C_{\mathbf{n}}(t)e^{i\omega t}, \tag{2}$$

$$C_{\mathbf{n}}(t) = \mathrm{Tr}\{\mathbf{d}_\perp(0)\cdot\mathbf{d}_\perp(t)\rho\}. \tag{3}$$

Here, the trace is performed over the atomic states and denotes a statistical average, ρ is the projection of the density operator onto the atom's Hilbert space evaluated at initial time, the brackets $\{...\}$ denote an average over the perturber trajectories (classical path approximation), and $\mathbf{d}_\perp = \mathbf{d} - (\mathbf{d}\cdot\mathbf{n})\mathbf{n}$ denotes the projection of the atomic dipole operator onto the polarization plane, in the Heisenberg picture. In Eq. (3), restrictions of this operator to the upper and lower levels of the transition are implied (no-quenching approximation). It is customary to write the autocorrelation function in terms of the evolution operator $U(t)$. Because of the identity $\mathbf{d}_\perp(t) \equiv U^\dagger(t)\mathbf{d}_\perp(0)U(t)$, a calculation of the line shape requires the knowledge of the matrix elements of $\mathbf{d}$ and an evaluation of $U(t)$. The evolution operator obeys the time-dependent Schrödinger equation

$$i\hbar\frac{dU}{dt}(t) = [H_0 + V(t)]U(t). \tag{4}$$

Here H_0 is the Hamiltonian including both the atomic energy level structure (with a non-Hermitian part accounting for natural broadening) and the Zeeman effect, and $V(t) = -\mathbf{d}\cdot\mathbf{F}(t)$ is the time-dependent Stark effect term (Schrödinger picture) resulting from the action of the microscopic electric field $\mathbf{F}(t)$. When this term is neglected, the Schrödinger equation has the trivial solution $U(t) = \exp(-iH_0t/\hbar)$, which shows, using Eqs. (3) and (2), that $I_0(\omega, \mathbf{n})$ reduces to a set of delta functions (or Lorentzian functions if the natural broadening is retained). By contrast, the case where $\mathbf{F}(t)$ has to be retained is much trickier because there is no general exact analytical solution. The time-dependent perturbation theory yields a formal expansion (Dyson series), which is not applicable in explicit calculations because of the non-commutation of the interaction term at different times (time-ordering problem). This concerns in particular the microfield due to ions. Several models, based on suitable approximations, have been developed in such a way to provide an analytical expression for the line shape (e.g., the impact and static approximations; the model microfield method; etc.). For

our purposes it is convenient to have a line shape model with less restrictive approximations, in such a way to make it applicable to various plasma conditions. A good candidate is the simulation technique [15] (see also the recent review in [17]).

3. The numerical simulation method

The purpose of "ab initio" simulations is to numerically reproduce the motion of the charged particles in the plasma so as to obtain the time dependent electric microfield $\mathbf{F}(t)$. While being CPU intensive, this method has the advantage of providing reference line shapes; e.g. it was used to test the accuracy of simpler analytical models like the unified theory or the model microfield method (see Fig. 1 for an illustration). Essentially, a numerical simulation consists of: (i) the calculation of a set of realizations for the electric field; (ii) the numerical integration of the Schrödinger equation for each realization; (iii) the average of the evolution operators on a set of realizations and the Fourier transform of the autocorrelation function. In the simulations performed for this work, we use a code [14] developed according to the method reported in [15, 16]. We consider that the ions move along straight line trajectories with constant velocities, sampled among the particles according to an equilibrium Maxwell distribution function. The electrons are not simulated here, but are described with an impact collision operator. The treatment of the correlations between ions and electrons is retained by using Debye screened fields. A cubic cell with periodic boundary conditions is considered. For each history of the electric field, the code solves the time dependent Schrödinger equation for the evolution operator $U(t)$ according to the algorithm $U(t + \Delta t) = U(t + \Delta t, t)U(t)$, with $U(t + \Delta t, t)$ being the infinitesimal evolution operator between times t and $t + \Delta t$. The latter operator is evaluated by a matrix exponential. We have calculated profiles of the Balmer γ line of deuterium (Dγ) for a set of densities, temperatures, and magnetic field strengths relevant to magnetic fusion edge plasmas, in such a way to provide a table that can be used in an analysis of experimental spectra (cf. enclosed zip file; for details on the use of the table see Appendix). The table provides Stark-Zeeman line shapes for equal ion and electron temperatures with values comprised between 0.316 and 31.6 eV, a plasma density ranging from 10^{13} to 10^{16} cm^{-3}, and a magnetic field up to 5 T. The Doppler broadening has not been retained [it can be accounted for through the convolution (1)]. The equal ion and electron temperatures as-

sumption is justified by the fact that the line shapes are weakly dependent on the temperature (see Fig. 2), which is in contrast to the density trend (Fig. 3; this trend is precisely the motivation for the elaboration of passive spectroscopy diagnostics involving Stark broadened lines). The magnetic field present in tokamaks yields a specific structure owing to the Zeeman effect, which is routinely observed on low-n Balmer lines (such as Dα). This structure is still present on Dγ but it tends to disappear as the density increases (Fig. 4). In general, the competition between the Stark and Zeeman effects is not straightforward. Figure 5 shows an example where the additional line broadening due to ion dynamics is much weaker when the Zeeman effect is taken into account. Qualitatively, this result stems from the fact that the Stark effect can act as a quadratic perturbation of the energy levels when the Zeeman effect is present (a similar argument was given in [14] regarding the impact approximation); however, this does not provide a quantitative estimate. A general analytical formula, describing the Stark broadening with account for ion dynamics (even in the absence of a B field), still remains to be derived. This task could employ extensions of already existing theoretical approaches such as the model microfield method (MMM) or the unified theory. Recent works were done with this aim, e.g. [20, 21]. Note that all the discussions above concern Doppler-free line shapes. If the density is not too large (typically less than 10^{14} cm^{-3}), the thermal motion of the emitters yields an additional broadening (Doppler effect), which can be comparable to the Stark and Zeeman effects (Fig. 6).

4. Application to spectra calculations

In the previous section, it has been shown that a reliable interpretation of hydrogenic spectral line shapes for diagnostics in tokamak edge and divertor plasmas should involve the use of accurate Stark models, even for lines with a low upper principal quantum number. An additional problem that occurs in applications is the non-uniformity of the emission zone along the line-of-sight. The formation of a spectral line results from the emission of atoms that are located in regions with different values of N, T_e etc., which renders the interpretation of spectra intricate. In recent years, modeling efforts have been carried out with the purpose of analyzing spectrum signals observed in a virtual plasma background obtained from a transport code (synthetic diagnostics, e.g. [22]). A major difficulty in this task is the elaboration of a line shape model sufficiently general and accurate to be applicable to the

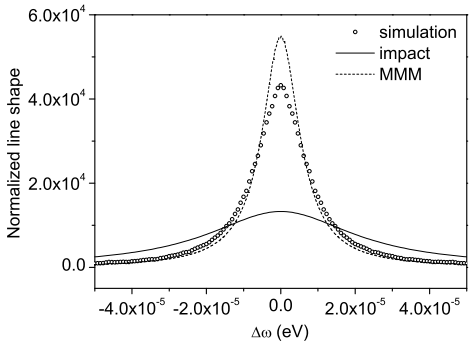

Figure 1: Simulations serve as a reference for testing the accuracy of simpler analytical models, especially regarding the description of ion dynamics. The standard impact theory applied to ions (e.g. [14]) usually overestimates the role of microfield dynamics and yields a line width larger than that obtained from a numerical simulation. This point is illustrated here for the Lyman α line of deuterium. A plasma density of 10^{14} cm^{-3} and ion and electron temperatures of 1 eV have been assumed in the calculation, and only the Stark broadening due to ions has been retained. Also shown in the figure is the result of the model microfield method (MMM), which is closer to the simulation but still deviates from it, in the opposite sense.

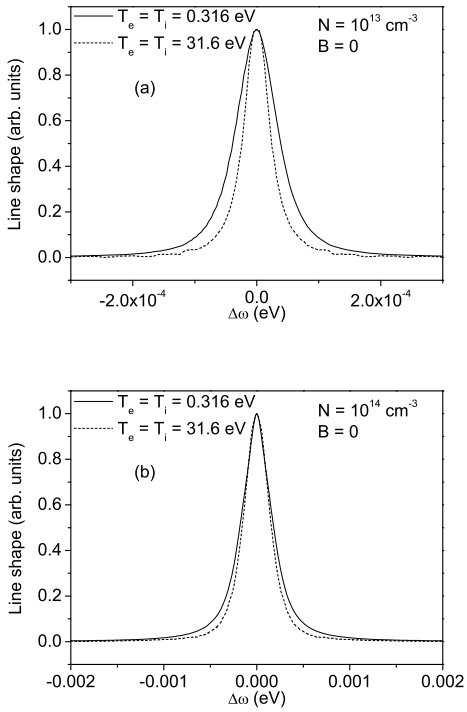

Figure 2: Plots of the Dγ line shape calculated at different temperatures. Setting two temperatures different by two orders of magnitude result in a relatively weak difference on the line width, typically by no more than 50%. The difference is even weaker as the density increases [compare (a) to (b)].

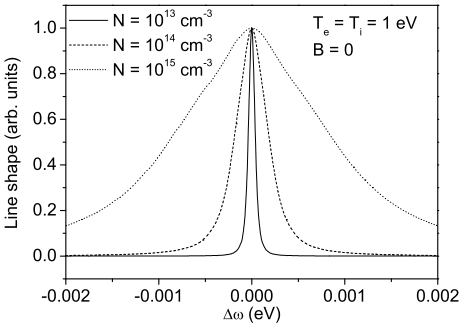

Figure 3: Plots of the Dγ line shape calculated at different densities. The line width has a strong (almost linear [19]) dependence on the plasma density N. It is precisely this trend that renders passive spectroscopy useful for the diagnostic of magnetic fusion edge plasmas.

(wide) range of values covered by the plasma parameters on the line-of-sight. Our database for Dγ (or any database obtained from the ab initio method discussed above) would provide an interesting approach because it involves no restrictive physical approximation on the atomic physics (namely: the time-dependent Schrödinger equation is solved) and it allows for a systematic evaluation of the emission spectra along the line-of-sight. As an illustration we show here an example of application to a virtual plasma background calculated from the SolEdge2D-EIRENE code [23] (see Fig. 7). Relevant values obtained for the divertor region include an electron density of the order of 10^{14} cm^{-3}, temperatures of several electron-volts, and a magnetic field of about 4.4 T. Given a line-of-sight crossing this plasma background, the following integral has been calculated:

$$\int_0^L ds N_{\rm at}(s) I(\omega, s). \tag{5}$$

Here, L is the length of the line-of-sight and s is a curvilinear coordinate that parameterizes the space dependence of the emission profile I along the line-of-sight. This dependence is implicit through the plasma parameters N, T_e etc. The quantity $N_{\rm at}$ denotes the density of atoms present in the excited state ($n = 5$); it also depends on space through the plasma parameters. We have evaluated this quantity from the same collisional-radiative model

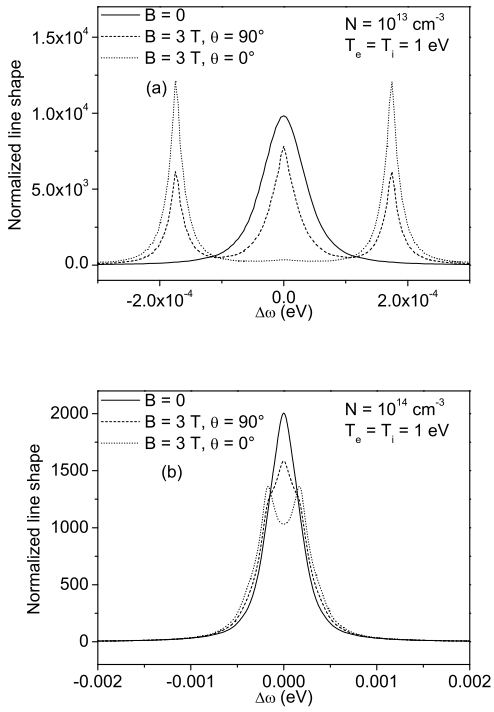

Figure 4: Plot of Dγ calculated assuming a magnetic field of 3 teslas, with an angle of 0° and 90° with respect to the observation direction. The same line shape calculated in an unmagnetized plasma is also shown. At low densities (a), the Zeeman effect yields a Lorentz triplet structure, with two or three peaks, depending on the observation direction. This structure diminishes as the density increases (b).

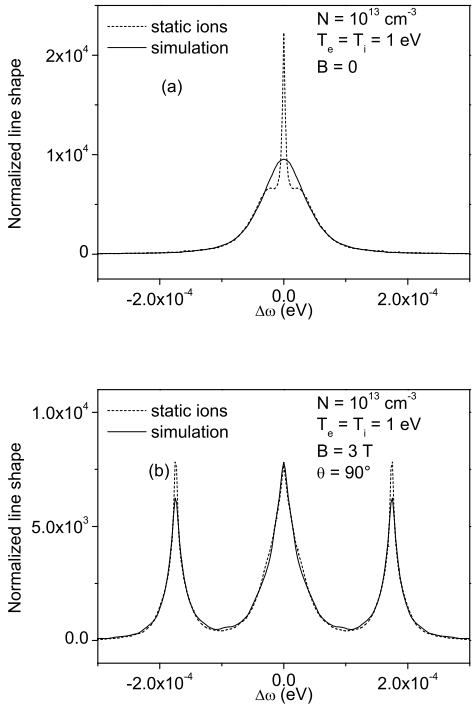

Figure 5: The ion dynamics provides an additional broadening, whose strength is determined by the magnetic field value. Here, plot of Dγ assuming (a) no magnetic field and (b) a magnetic field of 3 teslas. The calculation that assumes static ions was performed with the same code, formally setting the ions' velocities to zero.

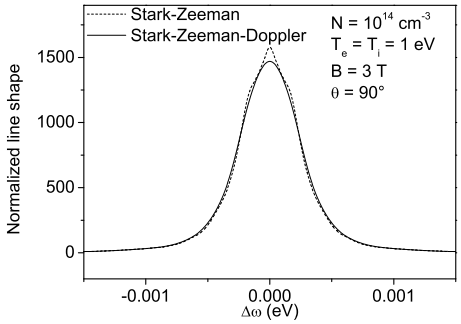

Figure 6: The Doppler and Stark broadenings can be of the same order of magnitude if the density is not too high. In this case, the Doppler effect masks the Stark-Zeeman structure.

as in [22]. Note, the propagation vector $\mathbf{n}$ is a constant and has not been written here for the sake of simplicity. We have calculated the integral (5) numerically. The local emissivity at each location on the line-of-sight has been evaluated from the database using a logarithmic interpolation for N, T_e, and a linear interpolation for B. Figure 8 shows the profile of Dγ observed from the third line-of-sight from the left in Fig. 7. No clear structure due to the Zeeman effect is visible here because the electron density on the line-of-sight is sufficiently high (typically larger than 10^{14} cm^{-3} at the region where the atomic density is the highest) and the Stark broadening is sufficiently strong so as to mask the Lorentz triplet structure. The local emissivity at the densest location, also shown in figure 8, is close to the apparent spectral profile, which suggests that the latter can serve as a diagnostic for the density at that location. A similar result was obtained for the hydrogen line spectra in the ITER divertor in high-density conditions in [22].

5. Conclusion

The operation of magnetic fusion devices requires passive spectroscopy diagnostics in the edge plasma region. In this work, we have elaborated a database for the interpretation of the hydrogen Balmer γ line in conditions of high-density recombining divertor plasmas. This database accounts for the simultaneous action of the Zeeman and Stark effects. The applicability of the database to diagnostics has been illustrated through spectra calculations

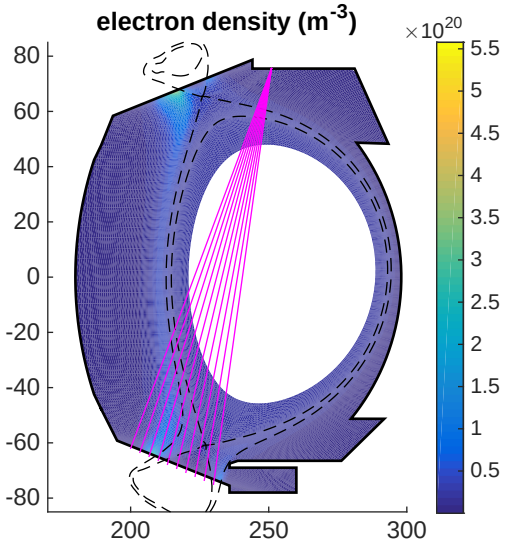

Figure 7: The line shape database can be used for the interpretation of spectra observed in a virtual plasma, i.e. resulting from a transport code (synthetic diagnostic). Here, this map gives an example of application to the WEST tokamak [24], an upgrade of Tore Supra currently under construction in Cadarache (France). Ten lines-of-sight crossing regions with different densities are shown. The coordinates in the x and y axes are expressed in cm.

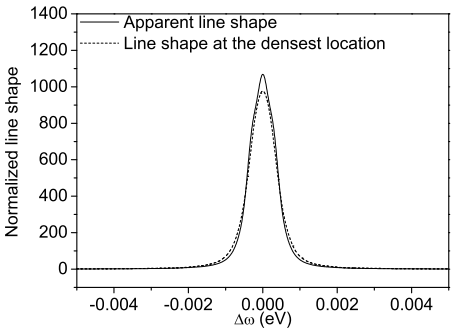

Figure 8: Plot of the apparent profile of Dγ, as it would result from a passive observation in the WEST divertor plasma. The spectrum, which involves an emission from plasma regions with different densities and temperatures, is close to the local emissivity at the densest location.

observed in a virtual plasma background obtained from a transport code. The results indicate that the "apparent" spectral profile as it results from line-of-sight integration can serve as a diagnostic for the electron density at the densest location. An extension of this work to the modeling of Balmer lines with a higher principal quantum number is currently in preparation. Applications to the analysis of experimental spectra will also be performed.

Acknowledgements

This work has been carried out within the framework of the EUROfusion Consortium and has received funding from the Euratom research and training programme 2014-2018 under grant agreement No 633053. The views and opinions expressed herein do not necessarily reflect those of the European Commission. Financial support was also received from the French National Research Agency (contract ANR-11-BS09-023).

Appendix

The enclosed zip file contains a set of line shapes calculated assuming the following parameters:

* $T_e = T_i = 0.316,\ 1,\ 3.16,\ 10,$ and 31.6 eV;
* $N = (1,\ 2.15,\ 4.64) \times (10^{13},\ 10^{14},\ 10^{15})$, and 10^{16} cm^{-3};
* $B = 0,\ 1,\ 2,\ 2.5,\ 3,$ and 5 T.

The folder contained in the zip file is organized as follows:
.\density\magnetic field\temperature. The files 'ls.txt', 'ls1.txt' denote the line shape in perpendicular and parallel observation, respectively. The line shape in any direction can be formed from $\cos^2\theta \times \mathrm{ls1} + \sin^2\theta \times \mathrm{ls}$, where θ is the angle between $\mathbf{B}$ and the line-of-sight. If $B = 0$, only 'ls.txt' is given. Each file 'ls.txt' or 'ls1.txt' contains a single area-normalized line profile. The first column is the photon energy detuning (eV). The second column is the intensity. The header gives the parameters (N, T, B). At $N \geq 4.64 \times 10^{14}$ cm^{-3}, the Stark effect is so important that there is no significant Zeeman splitting; hence, only the $B = 0$ results are given. The code uses the numerical simulation method described in Sec. 3. It was written for hydrogen isotopes in magnetic fusion edge plasmas [14, 22]. Note, the results here concern deuterium.

References

[1] S. Potzel, R. Dux, H. W. Müller, A. Scarabosio, M. Wischmeier, A. U. team, Plasma Phys. Control. Fusion 56 (2014) 025010.

[2] B. L. Welch, H. R. Griem, J. Terry, C. Kurz, B. LaBombard, B. Lipschultz, E. Marmar, G. McCracken, Phys. Plasmas 2 (1995) 4246.

[3] D. Lumma, J. L. Terry, B. Lipschultz, Phys. Plasmas 4 (1997) 2555.

[4] B. Lipschultz, J. L. Terry, C. Boswell, A. Hubbard, B. LaBombard, D. A. Pappas, Phys. Rev. Lett. 81 (1998) 1007.

[5] A. Y. Pigarov, J. L. Terry, B. Lipschultz, Plasma Phys. Control. Fusion 40 (1998) 2055.

[6] U. Wenzel, K. Behringer, A. Carlson, J. Gafert, B. Napiontek, A. Thoma, Nucl. Fusion 39 (1999) 873.

[7] D. Nishijima, U. Wenzel, K. Ohsumi, N. Ohno, Y. Uesugi, S. Takamura, Plasma Phys. Control. Fusion 44 (2002) 597.

[8] M. Koubiti, S. Loch, H. Capes, L. Godbert-Mouret, Y. Marandet, A. Meigs, R. Stamm, H. Summers, J. Quant. Spectrosc. Radiat. Transfer 81 (2003) 265.

[9] V. A. Soukhanovskii, D. W. Johnson, R. Kaita, A. L. Roquemore, Rev. Sci. Instrum. 77 (2006) 10F127.

[10] F. Scotti, V. A. Soukhanovskii, M. L. Adams, H. A. Scott, H. W. Kugel, R. Kaita, A. L. Roquemore, J. Nucl. Mater. 415 (2011) S405.

[11] J. Rosato, Y. Marandet, R. Stamm, J. Phys. B: At. Mol. Opt. Phys. 47 (2014) 105702.

[12] C. Stehlé, Astron. Astrophys. Suppl. Ser. 104 (1994) 509.

[13] A. Brissaud, U. Frisch, J. Quant. Spectrosc. Radiat. Transfer 11 (1971) 1767.

[14] J. Rosato, Y. Marandet, H. Capes, S. Ferri, C. Mossé, L. Godbert-Mouret, M. Koubiti, R. Stamm, Phys. Rev. E 79 (2009) 046408.

[15] R. Stamm, D. Voslamber, J. Quant. Spectrosc. Radiat. Transfer 22 (1979) 599.

[16] R. Stamm, E. W. Smith, B. Talin, Phys. Rev. A 30 (1984) 2039.

[17] E. Stambulchik, Y. Maron, High Energy Density Phys. 6 (2010) 9.

[18] E. Stambulchik, High Energy Density Phys. 9 (2013) 528.

[19] H. R. Griem, Spectral Line Broadening by Plasmas, Academic Press, London, 1974.

[20] H. Capes, M. Christova, D. Boland, F. Catoire, L. G.-M. M. Koubiti, A. Mekkaoui, J. Rosato, Y. Marandet, R. Stamm, AIP Conf. Proc. 1290 (2010) 104.

[21] J. Rosato, H. Capes, R. Stamm, Phys. Rev. E 86 (2012) 046407.

[22] J. Rosato, V. Kotov, D. Reiter, J. Phys. B: At. Mol. Opt. Phys. 43 (2010) 144024.

[23] H. Bufferand, et al., Nucl. Fusion, in press.

[24] J. Bucalossi, et al., Fusion Eng. Des. 89 (2014) 907.